Journal of Applied Mechanics and Technical Physics, Vol. 45, No. 4, pp. 598–604, 2004

COMPUTATIONAL-EXPERIMENTAL METHOD FOR DETERMINING FRACTURE PARAMETERS OF CRACKED STRUCTURES

V. N. Maksimenko and A. V. Tyagnii

UDC 539.375:629.7.02

Computational-experimental methods are proposed to estimate the mode I and II stress intensity factors, to determine the stresses acting at the location of a crack before its initiation, and to find the coordinates of the crack tips. The initial data are displacement discontinuities measured at several points at the crack edges. The methods are based on integral representations of the solution of the elastic equilibrium problem for anisotropic plates with a curved cut. Numerical examples are given to illustrate the efficiency of the methods.

Key words: *anisotropic plate, crack, displacement discontinuity, stress intensity factor.*

Methods based on experimental measurements of crack-opening displacements at several points are widely used to estimate the stress intensity factors (SIFs) at crack tips and to determine the stress distribution at crack locations before crack initiation [1–4]. These methods are applicable only to structures of isotropic materials and simple geometry (straight cracks).

In the present paper, using integral representations of the solutions of crack problems, we propose a general method for estimating the mode I and II SIFs at the tips of a curved crack and the stresses acting at the crack site before its initiation and a method for determining the coordinates of crack tips in complex plate structures from metallic or composite (anisotropic) materials from displacement discontinuities (openings) determined experimentally at several points at the crack edges.

1. Calculation of Stress Intensity Factors. We consider plane stresses in a plate from an elastic rectilinearly anisotropic (in particular case, isotropic) material with an internal through-thickness or edge crack L loaded by arbitrary external forces (P_1, P_2,... , P_j) (Fig. 1). The plate can be reinforced by stiffeners attached by means of rivets and/or glue transmitting shear forces. We assume that the crack edges are traction-free and do not interact with each other. Given the displacement discontinuity along the crack $G(t) = (u^+ - u^-) + i(v^+ - v^-) = g_1(t) + ig_2(t)$, it is required to determine the SIF.

According to [5], the stresses and displacements (except for rigid-body displacements) at an arbitrary point $z = x + iy$ in the plate are expressed in terms of the analytic functions $\Phi_\nu(z_\nu)$ and $\varphi_\nu(z_\nu)$ ($\nu = 1, 2$):

$$(\sigma_x, \tau_{xy}, \sigma_y) = 2\,\mathrm{Re}\Big\{\sum_{\nu=1}^{2}(\mu_\nu^2, -\mu_\nu, 1)\Phi_\nu(z_\nu)\Big\},$$

$$(u, v) = 2\,\mathrm{Re}\Big\{\sum_{\nu=1}^{2}(p_\nu, q_\nu)\varphi_\nu(z_\nu)\Big\}, \qquad \frac{d\varphi_\nu(z_\nu)}{dz_\nu} = \Phi_\nu(z_\nu). \tag{1.1}$$

Here $z_\nu = x + \mu_\nu y$, μ_ν are roots of the corresponding characteristic equation with positive imaginary parts and p_ν and q_ν are the constants of the plate material.

Novosibirsk State Technical University, Novosibirsk 630092. Translated from Prikladnaya Mekhanika i Tekhnicheskaya Fizika, Vol. 45, No. 4, pp. 168–175, July–August, 2004. Original article submitted March 25, 2003.

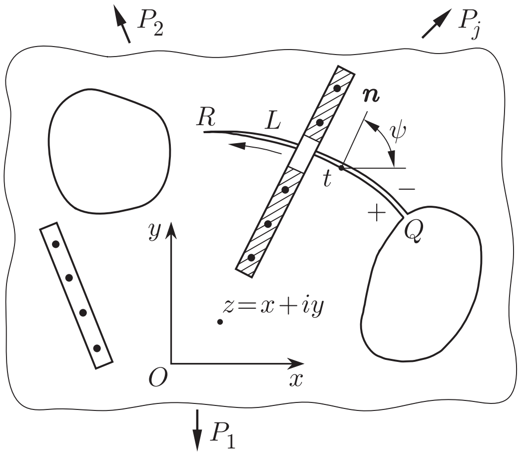

Fig. 1

Following [6], we write the functions $\Phi_\nu(z_\nu)$ as

$$\Phi_\nu(z_\nu) = \Phi_{\nu 0}(z_\nu) + \Phi_{\nu 1}(z_\nu); \tag{1.2}$$

$$\Phi_{\nu 1}(z_\nu) = \frac{1}{2\pi i} \int_L \frac{\omega_\nu(\tau)\, d\tau_\nu}{\tau_\nu - z_\nu}, \qquad \omega_2(t) = -a(t)\omega_1(t) - b(t)\overline{\omega_1(t)}, \tag{1.3}$$

where

$$a(t) = \frac{\mu_1 - \bar{\mu}_2}{\mu_2 - \bar{\mu}_2} \frac{M_1(t)}{M_2(t)}; \quad b(t) = \frac{\bar{\mu}_1 - \bar{\mu}_2}{\mu_2 - \bar{\mu}_2} \frac{\overline{M_1(t)}}{M_2(t)}; \quad M_\nu(t) = \mu_\nu \cos\psi - \sin\psi; \quad t, \tau \in L.$$

Here the functions $\Phi_{\nu 0}(z_\nu)$ define the principal stress state in the uncracked plate; the functions $\Phi_{\nu 1}(z_\nu)$ describe the disturbed stress state due to the presence of the crack L; $\psi(t)$ is the angle between the Ox axis and the normal $\boldsymbol{n}(t)$ to the point $t = x_t + iy_t$ at the left edge of the crack (Fig. 1); $\omega_\nu(t)$ are functions that have singularities of the square-root type at the internal tips of the crack L (i.e., tips that do not reach the plate edge or hole) [7], $\tau = x_\tau + iy_\tau$, and $\tau_\nu = x_\tau + \mu_\nu y_\tau$.

Using relations (1.1)–(1.3), we write the displacement discontinuity $G(t)$ in the form

$$G(t) = \sum_{\nu=1}^{2} \Big\{ (p_\nu + iq_\nu) \int_R^t \omega_\nu(\tau)\, d\tau_\nu + (\bar{p}_\nu + i\bar{q}_\nu) \int_R^t \overline{\omega_\nu(\tau)}\, d\bar{\tau}_\nu \Big\}.$$

Differentiating this relation with respect to the crack length s, we obtain the expressions of $\omega_1(t)$ in terms of the derivatives of g_1 and g_2:

$$\omega_1(t) = \frac{W(t)[A(t) - a(t)] - \overline{W(t)}\,[B(t) - b(t)]}{|A(t) - a(t)|^2 - |B(t) - b(t)|^2}, \tag{1.4}$$

where

$$W(t) = \frac{\bar{p}_2\, dg_2/ds - \bar{q}_2\, dg_1/ds}{(\bar{p}_2 q_2 - p_2\bar{q}_2) M_2(t)}; \quad A(t) = \frac{\bar{p}_2 q_1 - p_1 \bar{q}_2}{\bar{p}_2 q_2 - p_2 \bar{q}_2} \frac{M_1(t)}{M_2(t)}; \quad B(t) = \frac{\bar{p}_2 \bar{q}_1 - \bar{p}_1 \bar{q}_2}{\bar{p}_2 q_2 - p_2 \bar{q}_2} \frac{\overline{M_1(t)}}{M_2(t)}.$$

We consider the parametric equation of the contour L: $t = t(\alpha)$ and $\tau = t(\beta)$, where $-1 \leqslant \alpha \leqslant 1$, $-1 \leqslant \beta \leqslant 1$, $Q = t(-1)$, and $R = t(+1)$ for the internal crack and $0 \leqslant \alpha \leqslant 1$, $0 \leqslant \beta \leqslant 1$, $Q = t(0)$, and $R = t(+1)$ for the edge crack. In this case, the function $\omega_1(t)$ can be written as $\omega_1(t) = \omega_1[t(\alpha)] = \chi(\alpha)/(1 - \alpha^2)^{1/2}$. Here $\chi(\alpha)$ is a function of class H in the neighborhood of the point $\alpha = +1$ for the edge crack [7].

For the stresses in the neighborhood of the crack tips $c = t(\mp 1)$ [for an edge crack, $c = t(+1)$], using the results of [6], we obtain the asymptotic formulas

$$\lim_{r\to 0}\sqrt{2r}(\sigma_x,\tau_{xy},\sigma_y)=\operatorname{Re}\Big\{\sqrt{\pm\frac{ds}{d\alpha}\Big|_{\alpha=\mp 1}}\ \sum_{\nu=1}^{2}(\mu_\nu^2,-\mu_\nu,1)C_\nu(\vartheta)\Big\},$$

$$C_\nu(\vartheta)=\Lambda_\nu\sqrt{M_\nu(c)/(\cos\vartheta+\mu_\nu\sin\vartheta)},\qquad \Lambda_1=\chi(\mp 1),$$

$$\Lambda_2=-a(c)\Lambda_1-b(c)\bar\Lambda_1,\qquad s=s(\alpha),\qquad r=|z-c|,\qquad \vartheta=\operatorname{Arg}|z-c|$$

and the mode I and II SIFs, denoted by K_1 and K_2, respectively [8].

2. Determining Stresses at the Crack Location. For the cracked plate considered, we write the potentials $\Phi_\nu(z_\nu)$ as

$$\Phi_\nu(z_\nu)=\sum_{j=0}^{2}\Phi^*_{\nu j}(z_\nu). \tag{2.1}$$

Here $\Phi^*_{\nu 1}(z_\nu)=\Phi_{\nu 1}(z_\nu)$ and the potentials $\Phi^*_\nu(z_\nu)=\Phi^*_{\nu 1}(z_\nu)+\Phi^*_{\nu 2}(z_\nu)$ satisfy the following condition: the external loads applied to the body are nonzero only at the edges of the crack L. By virtue of the superposition principle, the potentials $\Phi^*_{\nu 0}(z_\nu)$ define the stresses in the intact plate, including the crack location.

The boundary conditions on L have the following form [6]:

$$a(t)\Phi_1^{\pm}(t_1)+b(t)\overline{\Phi_1^{\pm}(t_1)}+\Phi_2^{\pm}(t_2)=0,\qquad t_\nu=x_t+\mu_\nu y_t,\quad \nu=1,2. \tag{2.2}$$

Using the properties of the potentials $\Phi^*_{\nu 0}(z_\nu)$, from (1.3), (2.1), and (2.2) we obtain

$$X_n^*(t)+\bar\mu_2 Y_n^*(t)=(\bar\mu_2-\mu_2)M_2(t)[a(t)\Phi_1^*(t_1)+b(t)\overline{\Phi_1^*(t_1)}+\Phi_2^*(t_2)], \tag{2.3}$$

where $X_n^*(t)\,ds$ and $Y_n^*(t)\,ds$ are the components of the forces acting on the elementary arc ds of the contour L of the uncracked plate.

For three particular cases of the problem formulated above (an infinite plate with a crack, a half-plane with a crack, and an infinite plate with an elliptic hole), the functions $\Phi^*_\nu(z_\nu)$ can be written explicitly.

For an infinite plate with a crack L, we find that $\Phi^*_{\nu 2}(z_\nu)=0$. For a straight crack $L=\{|x|<a,\,y=\text{const}\}$, using (1.3), we obtain the following expression for the stresses σ_y^* and τ_{xy}^* that acted at the crack location before its initiation:

$$\tau^*_{xy}(x)+\bar\mu_2\sigma^*_y(x)=\frac{\bar\mu_2-\bar\mu_1}{\pi i}\int_{-a}^{a}\frac{\omega_1(\tau)\,d\tau}{\tau-x}.$$

For an internal or edge crack L located near the edge of a half-plane $D=\{x>0\}$, the functions $\Phi^*_{\nu 2}(z_\nu)$ should be written as follows [6]:

$$\Phi^*_{\nu 2}(z_\nu)=\frac{1}{2\pi i}\int_L\Big\{\frac{l_\nu s_\nu\overline{\omega_1(\tau)}\,d\bar\tau_1}{s_\nu z_\nu-\bar\tau_1}+\frac{n_\nu m_\nu\overline{\omega_2(\tau)}\,d\bar\tau_2}{m_\nu z_\nu-\bar\tau_2}\Big\}, \tag{2.4}$$

where

$$l_\nu=\frac{\mu_{3-\nu}-\bar\mu_1}{\mu_\nu-\mu_{3-\nu}};\quad n_\nu=\frac{\mu_{3-\nu}-\bar\mu_2}{\mu_\nu-\mu_{3-\nu}};\quad s_\nu=\frac{\bar\mu_1}{\mu_\nu};\quad m_\nu=\frac{\bar\mu_2}{\mu_\nu}\quad (\nu=1,2).$$

If a crack L is located near an elliptic hole $\Omega=\{(x/a)^2+(y/b)^2=1\}$ in an infinite plate or reaches the hole edge, the functions $\Phi^*_\nu(z_\nu)$ are given by [9]

$$\Phi^*_\nu(z_\nu)=\frac{d\zeta_\nu/dz_\nu}{2\pi i}\int_L\Big\{\frac{\omega_\nu(\tau)\,d\tau_\nu}{\zeta_\nu-\eta_\nu}+\frac{l_\nu\overline{\omega_1(\tau)}\,d\bar\tau_1}{\zeta_\nu(\zeta_\nu\bar\eta_1-1)}+\frac{n_\nu\overline{\omega_2(\tau)}\,d\bar\tau_2}{\zeta_\nu(\zeta_\nu\bar\eta_2-1)}\Big\}, \tag{2.5}$$

where

$$\zeta_\nu=\zeta_\nu(z_\nu)=(z_\nu+\sqrt{z_\nu^2-(a^2+\mu_\nu^2b^2)}\,)/(a-i\mu_\nu b);\qquad \eta_\nu=\zeta_\nu(\tau_\nu)\qquad(\nu=1,2).$$

The potentials $\Phi^*_\nu(z_\nu)$ defined by (2.4) and (2.5) automatically satisfy zero boundary conditions for the stresses at the edge of the half-plane or elliptic hole and at infinity.

3. Numerical Algorithm. Let the displacements discontinuities of the crack edges $g_{1p} = (u^+ - u^-)_p$ and $g_{2p} = (v^+ - v^-)_p$ be specified at N_1 and N_2 arbitrary points $t_{1p} = t(\alpha_{1p})$ and $t_{2p} = t(\alpha_{2p})$, respectively ($p = 1, \ldots, N_j$ and $j = 1, 2$). Taking into account the behavior of the function $\omega_1(t)$ and using relations (1.4), we approximate the displacement-discontinuity function $G(t)$ in the form of a series in the Chebyshev functions of the second kind $U_k(\alpha) = \sin(k \arccos\alpha)$ [10]

$$G(t) = G[t(\alpha)] = \sum_{k=1}^{M_1} b_{1k} U_k(\alpha) + i \sum_{k=1}^{M_2} b_{2k} U_k(\alpha). \tag{3.1}$$

Here b_{1k} ($k = 1, \ldots, M_1$) and b_{2k} ($k = 1, \ldots, M_2$) are unknown constants, which can be found by the least square method [10]. Minimization of the functional

$$S = \sum_{j=1}^{2} S_j, \qquad S_j = S_j(M_j) = \sum_{p=1}^{N_j} \Big[\sum_{k=1}^{M_j} b_{jk} U_k(\alpha_{jp}) - g_{jp}\Big]^2 \tag{3.2}$$

leads to the following two systems of linear algebraic equations for the coefficients of series (3.1):

$$\frac{\partial S}{\partial b_{jl}} = 2 \sum_{p=1}^{N_j} \Big[\sum_{k=1}^{M_j} b_{jk} U_k(\alpha_{jp}) - g_{jp}\Big] U_l(\alpha_{jp}) = 0 \qquad (l = 1, \ldots, M_j;\ j = 1, 2). \tag{3.3}$$

The optimal values of M_1 and M_2 for a finite number of points N_1 and N_2, respectively, can be evaluated with confidence level q using the condition that the criterion

$$J(M_j) = \frac{S_j(M_j)}{1 - \sqrt{\{M_j[\ln(N_j/M_j) + 1] - \ln(1-q)\}/N_j}} \qquad (j = 1, 2)$$

reaches the minimum positive value [11]. Here $S_j(M_j)$ are calculated by formula (3.2) for the coefficients b_{jk} determined from (3.3).

The derivatives of the displacement discontinuities dg_j/ds in (1.4) are expressed in terms of the Chebyshev functions of the first kind: $T_k(\alpha) = \cos(k \arccos\alpha)$ [10]

$$\frac{dg_j}{ds} = \frac{dg_j}{d\alpha}\frac{d\alpha}{ds} = -\frac{1}{\sqrt{1-\alpha^2}} \sum_{k=1}^{M_j} k b_{jk} T_k(\alpha) \Big(\frac{ds}{d\alpha}\Big)^{-1} \qquad (j = 1, 2).$$

To determine the forces (2.3) with allowance for (1.3), (2.1), (2.4), and (2.5), one can calculate the integrals at the nodal points α_m using the quadrature formulas for singular and regular integrals [12]

$$\int_{-1}^{1} \frac{V_1(\beta)\, d\beta}{\sqrt{1-\beta^2}\,(\beta - \alpha)} = \frac{\pi}{n} \sum_{k=1}^{n} \frac{V_1(\beta_k)}{\beta_k - \alpha_m}, \qquad \int_{-1}^{1} \frac{V_2(\alpha, \beta)\, d\beta}{\sqrt{1-\beta^2}} = \frac{\pi}{n} \sum_{k=1}^{n} V_2(\alpha, \beta_k), \tag{3.4}$$

$$\beta_k = \cos((2k-1)\pi/(2n)), \quad k = 1, \ldots, n; \qquad \alpha_m = \cos(\pi m/2), \qquad m = 1, \ldots, n-1.$$

For edge cracks, the integration interval $(0, 1)$ is replaced by the interval $(-1, 1)$ provided that $V_1(\beta) = 0$ and $V_2(\alpha, \beta) = 0$ for $\beta < 0$ and formulas (3.4) for even n are then used.

4. Determining the Crack Location. Let an internal straight crack be located along the Ox axis. We assume that the coordinates of the left and right tips of the crack (denoted by A and B, respectively) are unknown (for example, they have changed as a result of crack growth). Given the values of the displacement discontinuities $g_2 = v^+ - v^-$ at several points, it is required to determine the coordinates of A and B.

In this case, the approximation (3.1) becomes

$$G(x) = i g_2(x) = i \sum_{k=1}^{M_2} b_{2k} \sin\Big(k \arccos \frac{2x - B - A}{B - A}\Big). \tag{4.1}$$

To minimize the quantity $S = S_2$ in (3.2) with respect to the unknowns b_{2k}, B, and A, we have a system of nonlinear algebraic equations:

$$\frac{\partial S_2}{\partial b_{2k}} = 0 \quad (k = 1, \ldots, M_2), \qquad \frac{\partial S_2}{\partial B} = 0, \qquad \frac{\partial S_2}{\partial A} = 0. \tag{4.2}$$

To find the coordinate B of an edge crack $L = \{0 < x < B,\ y = \text{const}\}$, one can use system (4.2) eliminating the last equation and setting $A = -B$ in (4.1).

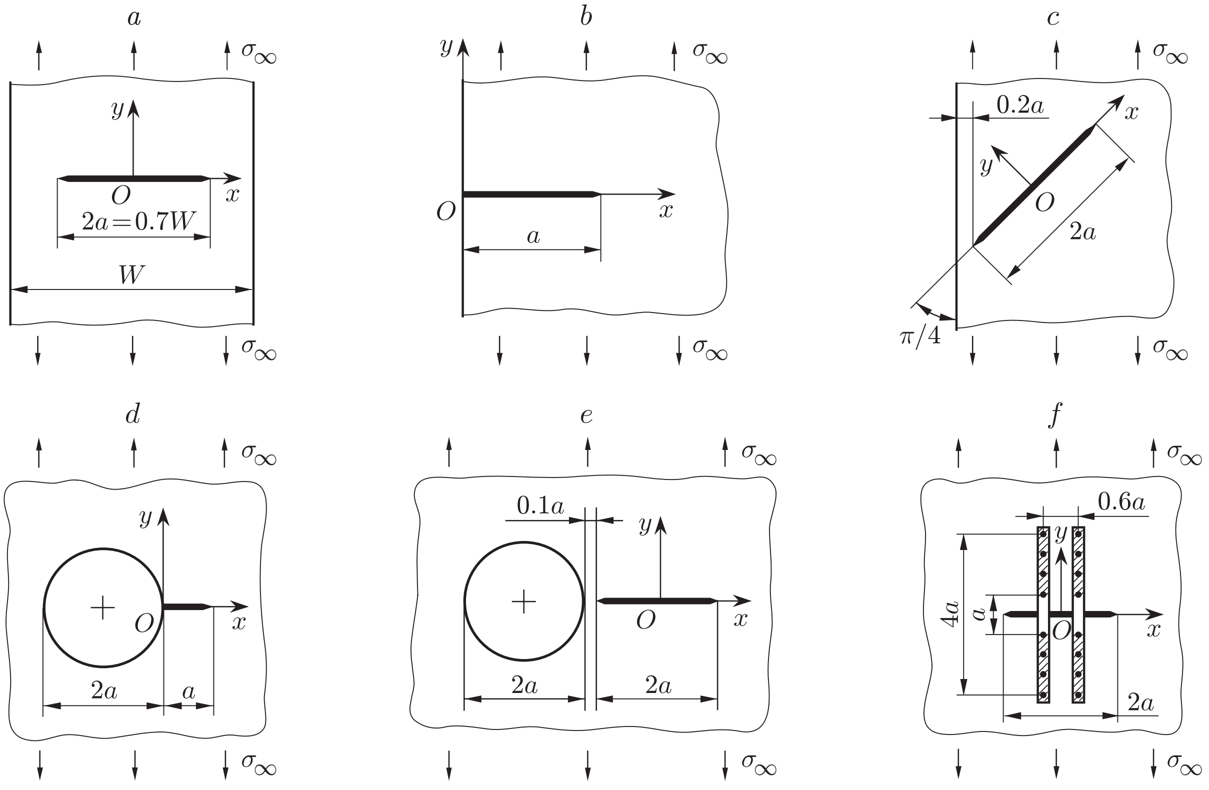

Fig. 2

5. Numerical Experiments. To illustrate the efficiency of the methods proposed, we consider the problems whose geometries and loading cases are shown in Fig. 2. Calculations were performed for an isotropic material modeled by an orthotropic material [5] with the following parameters: $E_x = E_y = E$, $\nu_{xy} = \nu_{yx} = 0.33$, and $G_{xy} = G_{yx} = 0.999E/[2(1 + \nu_{xy})]$ (E_x and E_y are Young's moduli along the principal Ox and Oy directions, respectively, G_{xy} and G_{yx} are the shear moduli, and ν_{xy} and ν_{yx} are Poisson's ratios). The geometrical parameters of the reinforced plate (Fig. 2f) are as follows: thickness of the isotropic plate $0.01a$, cross-sectional area of the reinforcing elements $0.002a^2$, elastic modulus of the elements E, glue thickness $0.001a$, shear modulus of the glue $0.01E$, splice thickness $0.1a$ [the splice is partly disrupted near the crack (delamination)], rivet diameter $0.04a$ (the rivets are located with a step of $0.5a$).

The numerical experiment was performed in two stages. In the first stage, the values of the displacement discontinuities and stress intensity factors $K^0_{1,2}$ were calculated for all problems in question using the integral-equation method [6, 9, 13] or the analytical solutions of [5, 8]. For the problems shown in Fig. 2b, c, and e, the stresses $\sigma^{*0}_y(x)$ and $\tau^{*0}_{xy}(x)$ at the crack location were also calculated. The error of the numerical solutions obtained by the integral-equation method was smaller than 0.1%. The displacement discontinuities were determined at one to seven points $\alpha_{jp} = [(2p - 1)/N_j] - 1$ (for internal cracks) or $\alpha_{jp} = (2p - 1)/(2N_j)$ (for edge cracks) located uniformly along the crack, where $p = 1, \ldots, N_j$ ($N_j = 1, \ldots, 5$) and $M_j = N_j$ ($j = 1, 2$). In the second stage, the displacement discontinuities obtained were used as initial data to calculate the SIF $K_{1,2}$, stresses at the crack location $\sigma^*_y(x)$ and $\tau^*_{xy}(x)$, and the crack-tip coordinates

Table 1 gives the relative errors for the mode I and II SIFs, ($N = N_1 = N_2$)

$$\delta_{1,2}(\pm a) = \{[K_{1,2}(\pm a) - K^0_{1,2}(\pm a)]/K^0_{1,2}(\pm a)\} \cdot 100\%,$$

and Table 2 gives the relative errors for the normal and shear stresses

$$\delta(\sigma_y) = \max_{x \in L_1} |[\sigma^*_y(x) - \sigma^{*0}_y(x)]/\sigma^{*0}_y(x)| \cdot 100\%, \qquad \delta(\tau_{xy}) = \max_{x \in L_1} |[\tau^*_{xy}(x) - \tau^{*0}_{xy}(x)]/\tau^{*0}_{xy}(x)| \cdot 100\%,$$

where $L_1 = \{-0.8 < x/a < 0.8\}$ for the internal crack and $L_1 = \{0.1 < x/a < 0.9\}$ for the edge crack.

TABLE 1

Relative Errors for the Mode I and II SIFs

Geometry shown in Fig. 2	E_x/E_y	Error	$N=1$	$N=2$	$N=3$	$N=4$	$N=5$
a	1	$\delta_1(+a)$	-3.3	-2.5	0.2	0.1	0.1
	1/25	$\delta_1(+a)$	3.3	-1.4	0.7	-0.3	0.3
	1/5	$\delta_1(+a)$	5.1	-2.0	0.8	-0.2	0.2
b	1	$\delta_1(+a)$	8.1	-2.8	1.0	-0.4	-0.2
	5	$\delta_1(+a)$	5.4	-2.2	0.9	-0.2	0.1
	25	$\delta_1(+a)$	3.3	-1.5	0.6	-0.3	0.2
	1	$\delta_1(-a)$	16.7	26.4	16,7	7.9	3.0
c	1	$\delta_2(-a)$	-29.1	-12.3	-1.8	1.7	2.3
	1	$\delta_1(+a)$	13.9	1.0	-3.5	2.2	-1.2
	1	$\delta_2(+a)$	8.0	-8.6	3.7	-1.0	0.1
d	1	$\delta_1(+a)$	9.6	-3.1	1.0	-0.3	0.2
e	1	$\delta_1(-a)$	-36.2	-19.7	-9.9	-4.5	-1.6
	1	$\delta_1(+a)$	13.0	-7.5	4.3	-2.2	1.2
f	1	$\delta_1(+a)$	-20.7	-14.5	4.7	4.5	4,0

TABLE 2

Relative Errors for the Normal and Shear Stresses

Geometry shown in Fig. 2	E_x/E_y	Error	$N=1$	$N=2$	$N=3$	$N=4$	$N=5$
	1/25	$\delta(\sigma_y)$	15.3	6.7	4.7	2.8	1.5
	1/5	$\delta(\sigma_y)$	28.1	9.3	4.3	1.4	0.7
b	1	$\delta(\sigma_y)$	38.0	11.2	4.0	1.1	0.5
	5	$\delta(\sigma_y)$	29.3	9.6	4.2	1.5	0.8
	25	$\delta(\sigma_y)$	15.5	6.7	4.7	2.9	1.7
c	1	$\delta(\sigma_y)$	30.4	27.1	12.0	6.9	3.3
e	1	$\delta(\sigma_y)$	49.5	23.8	8.8	4.6	2.2

TABLE 3

Relative Errors for the Crack-Tip Coordinates

Geometry shown in Fig. 2	Error	$M_2=1$	$M_2=2$	$M_2=3$	$M_2=4$	$M_2=5$
d	$\delta(B)$	-0.8	4.1	-1.0	0.4	0,1
e	$\delta(A)$	34.0	14.0	6.0	2.6	1.2
	$\delta(B)$	-3.6	3.0	-1.4	1.0	-0.5

For the case shown in Fig. 2b, the convergence of the solution (for the SIFs and stresses) was studied for various degrees of anisotropy of the material. The calculations were performed for $E_x/E_y = 1/25$, 1/5, 1, 5, and 25, $G_{xy} = G_{yx} = 0.999 \min(E_x, E_y)/[2(1 + \max(\nu_{xy}, \nu_{yx}))]$, where $\max(\nu_{xy}, \nu_{yx}) = 0.33$ and $\nu_{xy}/E_x = \nu_{yx}/E_y$. The results show that two or five measurement points are sufficient to reach an error not exceeding 3–4% in determining the SIF $K_{1,2}$ and stresses σ_y^* and τ_{xy}^* in typical structural members for a wide range of the anisotropy of the material. This indicates good convergence of the method.

The crack-tip coordinates determined by the method described in Sec. 4 are given in Table 3. The error for the coordinates of the crack tips $\delta(A, B) = [|(A, B)/a| - 1] \cdot 100\%$ was calculated for $M_2 = 1, \ldots, 5$ and $N_2 = M_2 + 1$ for edge cracks and $N_2 = M_2 + 2$ for internal cracks (the points were located uniformly along the crack). For the most complex case (the left crack tip in Fig. 2e), the error $\delta(A)$ did not exceed 1.2% for $M_2 = 5$ and $N_2 = 7$.

The numerical studies performed show that the methods proposed here are effective for the analysis of the stress-strain state of cracked structures based on experimental data.

REFERENCES

1. V. I. Gorodnichenko and A. D. Dement'ev, "Evaluation of the stress intensity factors at the tip of a through-thickness crack from displacement fields," *Uch. Zap. TsAGI*, **19**, No. 6, 82–93 (1989).
2. S. V. Shkaraev, "Theoretical-experimental method for determining the stress intensity factors," *Fiz. Khim. Mekh. Mater.*, No. 4, 97–101 (1989).
3. S. V. Shkaraev, "Method for evaluating the fracture parameters of structural members with edge cracks," factors," *Fiz.-Khim. Mekh. Mater.*, No. 6, 29–35 (1992).
4. T. Torri, K. Houda, T. Fujibayashi, and T. Hamano, "A method of evaluating crack opening stress distributions and stress intensity factors based on opening displacement along a crack," *JASM Int. J., Ser. I*, **32**, No. 2, 47–54 (1990).
5. S. G. Lekhnitskii, *Anisotropic Plates*, Gordon and Breach, New York (1968).
6. V. N. Maksimenko, "Problem of a crack in an anisotropic half-plane reinforced by elastic patches," in: *Dynamics of Continuous Media* (collected scientific papers) [in Russian], No. 99, Inst. of Hydrodynamics, Sib. Div., Russian Acad. of Sci., Novosibirsk (1990), pp. 41–46.
7. F. D. Gakhov, *Boundary-Value Problems* [in Russian], Fizmatgiz, Moscow (1963).
8. V. V. Panasyuk (ed.), *Fracture Mechanics and Strength of Materials* [in Russian], Vol. 2, Naukova Dumka, Kiev (1988).
9. V. N. Maksimenko, "Limit equilibrium of an anisotropic plate weakened by an elliptic hole and cracks of complex shape," *Uch. Zap. TsAGI*, **18**, No. 3, 24–29 (1987).
10. I. S. Berezin and N. P. Zhidkov, *Calculation Methods*[in Russian], Vol. 1, Nauka, Moscow (1966).
11. V. N. Vapnik, *Algorithms and Programs for Finding Dependences* [in Russian], Nauka, Moscow (1984).
12. S. M. Belotserkovskii and I. K. Lifanov, *Numerical Methods in Singular Integral Equations* [in Russian], Nauka, Moscow (1985).
13. V. N. Maksimenko and V. N. Pavshok, "Calculation of a cracked anisotropic plate strengthened with fastened and bonded ribs," *J. Appl. Mech. Tech. Phys.*, No. 1, 118–124 (1992).